American Journal of Materials Engineering and Technology, 2021, Vol. 9, No. 1, 21-30
Available online at http://pubs.sciepub.com/materials/9/1/2
Published by Science and Education Publishing
DOI:10.12691/materials-9-1-2

Elaboration of Porous Geopolymer Cement from Sangaré Clay and Shell Egg Powder: Application as Thermal Insulation

Jeanne Atchana[1,2,*], Paul Nestor Djomou Djonga[1], Benoit Loura[2], Valery Gomdje Hambate[3], Jean Bosco Tchatchueng[4]

[1]Department of Chemistry, Faculty of Science, University of Maroua, P.O. Box 46 Maroua, Cameroon
[2]Department of Refining and Petrochemistry, P.O. Box 08, University of Maroua, Kaele Cameroon
[3]Departement of Textile and Leather Engineering, National Advanced School of Engineering of Maroua, University of Maroua, P.O. Box 46 Maroua, Cameroon
[4]Department of Applied Chemistry, National Advanced School of Agro Industrial Food, University of Ngaoundere, P.O. Box 455Ngaoundere, Cameroon
*Corresponding author: atjeane@yahoo.fr

Received September 10, 2021; Revised October 14, 2021; Accepted October 24, 2021

Abstract This study focuses on the preparation of porous geopolymer cements for thermal insulation applications using commercial calcium carbonate and low-value calcium carbonate-rich waste such as eggshell powders as pore-forming agents. The control and porous geopolymer cements were prepared by adding phosphoric acid (4M) as a chemical ingredient to metakaolin containing 0 and 10 wt% of the foaming agent. Results showed that Sangare clay is sandy with a few silts and traces of gravel. Diffractogram of the clay indicates the presence of: Kaolinite (Kao); Illite (Ill); Quartz (Qz) and Potassium Feldspars (Fds). This was confirmed by the Infrared spectrum of the material where bands characteristic of the presence of kaolinite (3689-3649 cm $^{-1}$) and of other minerals have been found. Characterization of eggshell powder shows that the source of calcium consists mainly of $CaCO_3$. The apparent densities of geopolymer cement obtained decreased when the aluminosilicate materials (metakaolin) are replaced by proportions of eggshell powders and commercial calcium carbonate (0, 1, 3, 5, 7 and 10%). It was also observed that the compressive strengths of geopolymer cements based on eggshells are greater than those based on commercial calcium carbonate and the thermal conductivity decreases with the increase of the porogen. These results corroborates with that of the apparent density and compressive strength which decreases with the increase of the porogen. Results shows that geopolymer cements obtained have accumulated high pores in their structures. The values of thermal conductivity of the control and porous geopolymer cement from eggshell ranges between 0.10 and 0.17 W/mK, respectively. It was concluded that the low-value calcium carbonate-rich wastes (egg shell) could be used for producing porous geopolymer cements which could be utilized for thermal insulation applications.

Keywords: *Sangaré clay, egg shell, thermal insulator and porous geopolymers*

Cite This Article: Jeanne Atchana, Paul Nestor Djomou Djonga, Benoit Loura, Valery Gomdje Hambate, and Jean Bosco Tchatchueng, "Elaboration of Porous Geopolymer Cement from Sangaré Clay and Shell Egg Powder: Application as Thermal Insulation." *American Journal of Materials Engineering and Technology*, vol. 9, no. 1 (2021): 21-30. doi: 10.12691/materials-9-1-2.

1. Introduction

The term geopolymer was first introduced in 1979 by Professor Joseph Davidovits. He defines it as a class of semi-crystalline aluminosilicate material with a three-dimensional network, obtained by mixing an aluminosilicate powder with a hardener [1]. The hardener generally used geopolymers are solutions of sodium or potassium silicate and a solution of phosphoric acid [1,2,3,4]. The work carried out on geopolymers for more than two decades is oriented in the construction of large buildings. Little work has been done on the synthesis of porous geopolymer cements, although the latter find applications in eco-construction [5], adsorption [6,7], catalysis [8], water absorption [9,10]. The porous geopolymer materials are synthesized in the same way as those which do not contain pores with the only difference that in addition to the hardener, a pore-forming agent which can be a powder or a solution is added to the aluminosilicate material. The pore-forming agents generally used for the synthesis of porous geopolymer materials in an alkaline medium are aluminum powder [11,12], silica fume [13], hydrogen peroxide [1,14,15,16], sodium perborate [17]. These pore-forming agents used by these authors are expensive. It is important to note that these authors used metakaolin as a source of aluminosilicate for the production of porous materials.

Previous work has shown that the non-porous geopolymeric materials synthesized from metakaolin have properties far superior to those obtained from volcanic slag [18]. This is due to the low reactivity of volcanic slag compared to that of metakaolin. This low reactivity is linked to a low specific surface area of volcanic slag (2.3 or 15.7 m^2/g) compared to that of metakaolin (20.5m^2/g) [18]. Recycling of natural waste such as eggshells, oyster shells, snail shells, rice husk ash, wheat ash, etc. offers many economic and environmental benefits, as it reduces disposal costs in landfills and maintains a healthy environment. Eggshells have a high content of calcium carbonate and until today, this waste is not yet used as a pore-forming agent for the production of porous geopolymer materials in acidic and/or alkaline media. The main goal of this work is to use eggshell powders as a pore-forming agent and garoua sangaré clay for the preparation of porous geopolymer cements and then compared the properties of these materials to those obtained using calcium commercial carbonate.

2. Literature Review

Some researchers [19,20] have concluded that geopolymeric materials are characterized by their low thermal conductivity, low compressive strength and low bulk density. The blowing agents commonly used for the production of porous geopolymer cements are aluminum powder [19,20,21], hydrogen peroxide [1,22], silica fume [23], the sodium perborate [17,24] used glass powders to prepare porous geopolymers and eggshell powders were used as blowing agents [25] used eggshells [26] prepared porous geopolymeric cements based on phosphoric acid using limestone as a pore-forming agent. It is important to indicate that these authors studied the thermal behavior of porous geopolymer cements up to 1000°C.

3. Material and methods

3.1. Presentation of the Study Area

During the construction of a well for access to underground water, a strange observation was made. On a lateritic horizon, at a depth of about 3 m, we notice the appearance of a layer of soil of a whitish and greyish color, layer of soil to which we pay all the interest of this work. The objective of this part is to present the major features of the studied area. Regarding soils, the parent material is mainly composed of clay and sand.

3.2. Geological Context

Geologically, Garoua is based on sedimentary formations mainly sandstone which is a detrital rock formed in the Cretaceous and resulting from the aggregation of grains of sand [27]. There is also the presence of massifs of gneiss which is a metamorphic rock composed of quartz, mica and feldspars. Sudanese tropical climate of the region combined with the presence of a river leads to the alteration of parent rocks and the formation of lacustrine clays [28] dating from the Quaternary period which sediment in alluvium, eluvium and are sometimes covered with a humic horizon and lateritic.

3.3. Material Sampling

On the whitish and grayish soil layer extracted from the well, a sampling targeted at the point of coordinates in decimal degrees, Latitude 9.285126° and Longitude 13.455767° was carried out. More attention was paid to the compact and gray masses of uncontaminated soil which crumbled to the touch because the other fraction of completely whitish soil was macroscopically only sand. Documentary studies [27] suggested the clayey nature of this greyish material (Figure 1). The samples taken are shown in Figure 2.

Figure 1. View of the situation at the sampling point (Well)

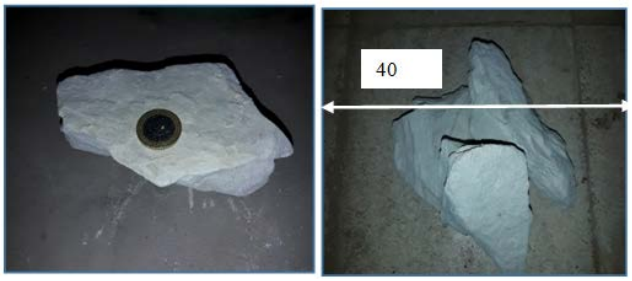

Figure 2. Presentation of the samples taken

3.4. Particle Size Analysis

The particle size analysis determines the dimensional distribution by weight of the grains constituting the sample.

3.5. Mineralogical Analyzes

They include X-Ray Diffractometry (XRD) and Infrared Spectrometry (IR).

3.6. Pore-forming Agents

The sources of calcium carbonate used are commercial calcium carbonate and chicken eggshells. For this study, the shells were collected in municipal landfills in Maroua. These shells, are washed with tap water, air dried and then broken by hand into small particles (about 2-4 mm). Before use, the organic material was removed and the shells devoid of this organic material were air-dried, then calcined at 500°C for 2 hours in a programmable electric oven (Nabertherm, Mod. LH 60/14), according to a heating rate of 10°C/ min. Then, it was ground using an AMS brand ball mill to obtain the powder. The powder was sieved until full passage through a 80 µm mesh sieve. Commercial calcium carbonate was supplied by Sigma-Aldrich.

4. Experimental Methods

4.1. Preparation of the Hardener

The hardener is obtained by diluting the commercial solution of phosphoric acid (H_3 PO_4, 85% purity) in distilled water in order to obtain a solution of molar concentration 4 M. The hardener thus prepared is left at room temperature for at least 24 hours before use.

4.2. Geopolymer Cement Production Process

The fresh geopolymer cement paste is obtained by gradually adding the hardener to the previously calcined clay (metakaolin) containing 0 and 15% by mass of each source of calcium in a porcelain mortar. The liquid / solid mass ratio is maintained at 0.83. The different formulations are then mixed manually for 5 minutes. The geopolymer cement pastes obtained by each formulation are molded in cubic (40 x 40 x 40 mm) and rectangular (40 x 40 x 15 mm plexiglass and cylindrical (63 x 30 mm) molds. The test pieces are then placed in a Genlab. Prime brand oven at 65°C for 24 h in order to accelerate the polycondensation process. The geopolymer cement bricks obtained are demolded, then sealed in plastics and left at room temperature (25±1) °C with a humidity of (55 ± 5) %, for 28 days.

4.3. Characterization Methods of Raw Materials and Geopolymer Cements Technical Characterization

The chemical composition of Sangare clay, egg shell powder and geopolymer cement was analyzed using a wavelength dispersive X-ray fluorescence apparatus (Shimadzu XRF-1800). In addition, X-ray diffraction (D RX) analysis was performed to test the mineralogical category using a Philips X'Pert PRO diffractometer equipped with a Ni- filtered Cu-Ka ($\lambda = 1.542$Å) radiation. Thermogravimetric analysis (TGA) and differential scanning calorimetry (DSC) analyzes were performed using a 2960 TA Instrument under argon from room temperature up to 1000°C at a heating rate of 5°C / min. The microstructures of the cement were analyzed by scanning electron microscopy (SEM) (Hitachi S-4500). The particle size distributions of the various obtained geopolymer powders were measured using a laser diffraction particle size analyzer (Malvern Mastersizer 2000). Infrared spectroscopy (FTIR, iS50 RAMAN) was used to identify some surface groups.

4.3.1. Measurement of Bulk Density

This measurement was made by the Archimedes thrust method using an automatic density meter (Ceramic Instruments mod DDA/2). This analysis was carried out in the Civil Engineering Laboratory of Cameroon.

4.3.2. Measurement of Compressive Strength

Compressive strengths were measured by crushingcubic molds (40 x 40 x 40 mm) of cured geopolymer materials, maintained at room temperature in the laboratory for 28 days. The test consists of subjecting the specimen between two opposing axial forces, located between the plates of the electrohydraulic press (IMPACT TEST Limited, Building 21, Stevenston Industrial Estate, Stevenston, Ayrshire, Scotland, UK KA2 0 3LR). Subsequently, the sample will be subjected to a continuous and progressive load at the average speed of 0.500 MPa/s until crushing. This analysis was carried out in the Civil Engineering Laboratory of Cameroon.

4.3.3. Optical Microscopy

The fragments of different géolpolymèr samples were used for light microscopy. It was made using an optical microscope equipped with a stereo microscope (Ceramic Instruments, Model 101T-M7), a binocular head and a tablet 7 with integrated micro camera. This analysis was carried out in the Civil Engineering Laboratory of Cameroon.

4.3.4. Mercury Intrusion Porosimetry

Mercury intrusion porosimetry (MIP) was performed on fragments of samples of approximately 1cm^3 in volume using an Autopore IV MIP 9500, 33,000 Psia (228MPa) covering the pore diameter range of about 0.006 to 350 µm having two low pressure ports and one high pressure chamber.

4.3.5. Measurement of Thermal Conductivity

Thermal conductivity is an analysis that studies the diffusion of energy within a material. The method is based on the use of a transient plane sensor, the most common adaptation of which is the Hot Disk thermal properties analyzer. The specimens produced for this analysis are cylindrical specimens of dimensions (63 x 30 mm).

5. Results and Discussion

5.1. Characterization of the Clay Precursor

These results concern the geotechnical, physical, mineralogical characterization and global evaluation of the properties of the Sangaré clay material once transformed into ceramics.

Particle size analysis

Table 1. Granulometric analysis of the clay material of Sangaré

Proportion of materials **(%)**				
(%) engravings	(%) sand	(%) slit	(%) clay	Total
d<2000µm	20< d<2000µm	2< d<20µm	d<2µm	
0.53	41.15	12.28	46.04	100

The granulometric analysis data are grouped in Table 1. The clay material consists of 0.53% gravel, 41.15% sand, and 12.28% silt and 46.04% clay. It is apparent from the exploitation of the results that the Sangare clay material has a very wide granulometry because its uniformity coefficient is greater than 200. It is sandy clay with a few silts and traces of gravel.

Mineralogical analyzes

i) X-ray diffractometry

Examination of the total powder diffractogram obtained for the sample tested shows the presence of the following minerals with the inter-reticular distances of their main lines: Kaolinite (Kao): reflection at 7.17 Å, 1.48 Å,

3.576 Å; Illite (Ill): reflection at 9.995 Å, 4.996 Å, 4.45 Å; Quartz (Qz): reflection at 4.255 Å, 3.343 Å, 1.81 Å; Potassium Feldspars (Fds): reflection at 3.240 Å, 2.753 Å, 2.159 Å. We also note the presence of the peak corresponding to the total clay inter-reticular distance at 4.45 Å. At this peak, all clay minerals were found.

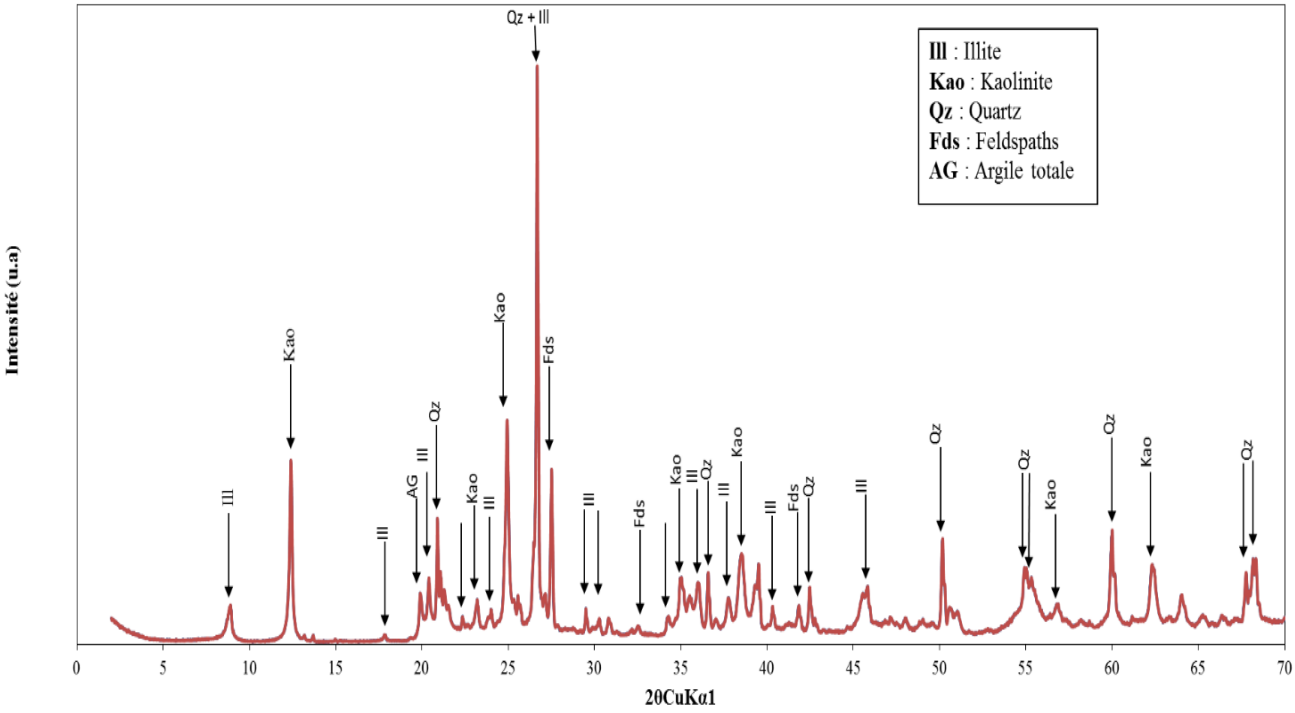

Figure 3. Diffractogram with total clay powder

Figure 3 shows the oriented blade curves obtained from the clay fraction less than 2 microns. The diffractogram obtained on the normal powder shows the presence of kaolinite and illite.

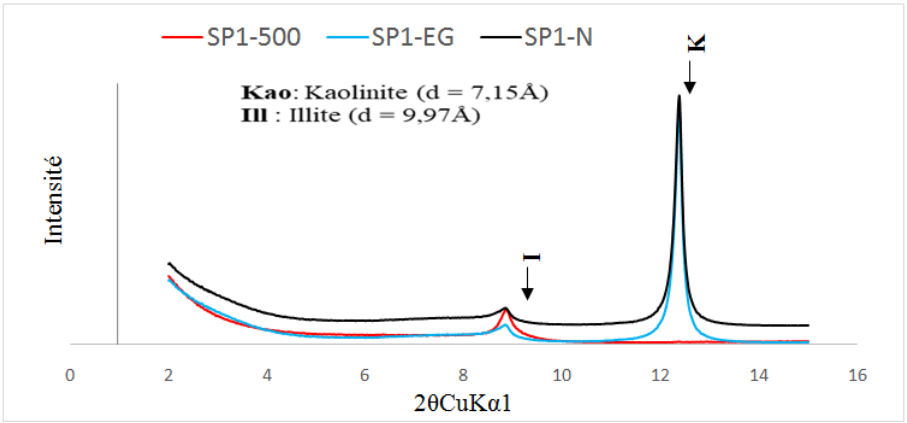

Figure 4. Diffractogram obtained in preparation oriented on clay fraction

In order not to make an identification error in the event that there would be clay minerals in the neighboring interfollial space in the normal powder, a diffractometry was also carried out on an oriented slide after heating to 500°C (SP1-500°C). The obtained diffractogram shows that the peak of kaolinite detected on the diffractogram of the normal oriented plate disappears, which confirms that it is indeed kaolinite because it is very sensitive to heat. Illite is present with a significant peak of inter-reticular distance 9.97 Å. The ethylene glycol (SP1-EG) saturation of the clay fraction on an oriented slide shows the absence of interbedded clay minerals. The calcination of the kaolin will make it possible to obtain metakaolin which will be used subsequently for the production of cement.

ii) Infrared spectrometry

In the clay material, bands characteristic of the presence of kaolinite (3689-3649 cm^{-1}) have been found because the valence vibrations of four OH groups composing the elementary mesh of kaolinite result in four bands centered at 3695, 3667, 3651, and 3620 cm^{-1} [29]. The 3619 cm^{-1} band reflects the OH bond deformation and materializes the presence of kaolinite [29]. The 1114 cm^{-1} band and the 1004 cm^{-1} band correspond to the elongation vibration of the Si-O bond of kaolinite. The bands observed around 914 and 916 cm^{-1} correspond to the deformation vibrations of the Al-O bond of the clay minerals [30]. The presence of Quartz is indicated by bands between 600 and 800 cm^{-1} [31]. Figure 5 crosses the bands between 3500 and 4000 cm^{-1} of the infrared spectrum

and corresponding to the main vibrations characteristic of kaolinite.

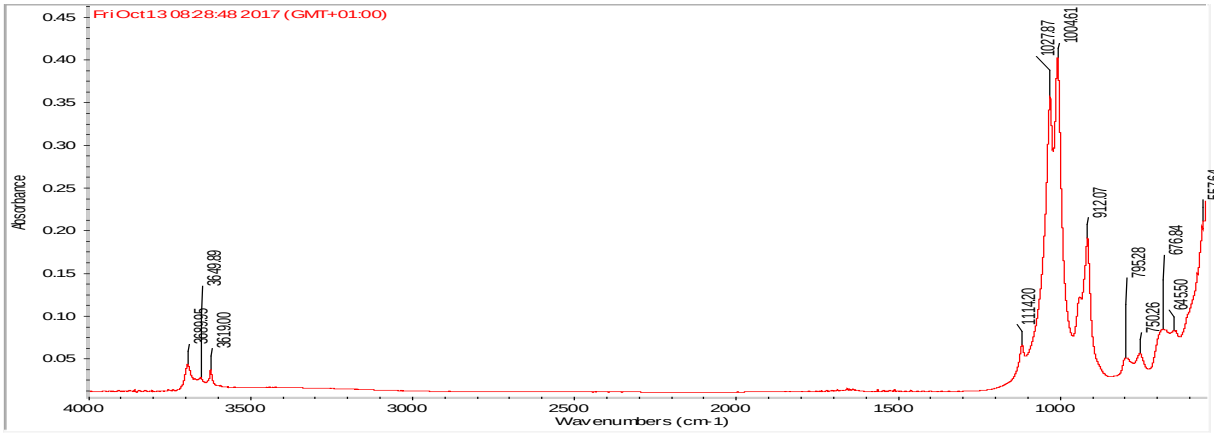

Figure 5. Infrared spectrum of the analyzed material

Table 2. Bands of the IR spectrum corresponding to the main minerals present in the clay material of Sangaré

Wavenumber (in cm $^{-1}$)	Matching bands
3689	Vibration of elongation of the external hydroxyl (OH) bonds of the Kaolinite network (Al-OH-Al)
3649	Valence vibration of the OH group composing the elementary cell kaolinite
3619	Vibration of elongation of hydroxyl bonds (OH) materializing the presence of kaolinite
1114	Vibration of the Si-O bond of kaolinite.
1027	Deformation vibration of the Al-O-Al bonds of kaolinite
1004	Kaolinite Si-O bond elongation vibration
912	Kaolinite Si-O bond elongation vibration
795 750	Vibration characteristics of the SiO4 group of Quartz vibration of the Si-O-Al bond of kaolinite
676 645	Vibration characteristic of the SiO4 group of Kaolinite and Quartz

Table 3. Mass chemical compositions of hen eggshells (ES), calcium carbonate (CC) and obtained Metakaolin (MKS), (LF: Loss on Fire)

Oxides	Na_2O	MgO	Al_2O_3	SiO_2	P_2O_5	SO_3	K_2O	$CaCO_3$	TiO_2	Cl^-	Fe_2O_3	ZnO	SrO	Ace $_2$ O $_3$	LF
ES	0.136	0.855	0.233	0.243	0.476	0.206	0.071	93.166		/	0.085	/	0.288	/	/
CC	/	/	/	0.19	/	/	/	99. 35	/	/	/	/	/	/	/
MKS	/	/	32.56	47.23	0.36	0.02	1.02	/	2.91	/	0.76	/	/	/	12.36

5.2. Characterization of Eggshell Powder

Chemical compositions (mass/100g)

The chemical compositions expressed in percentages by weight of oxides of the raw materials used such as the hen egg shells (ES) is recorded in Table 3. It emerges from this Table that the chemical composition of snail shells (SS) and commercial calcium carbonate (CC) has a high content of $CaCO_3$ (98.39%). The results show that these sources of calcium consist mainly of $CaCO_3$.

It emerges from this table that the chemical composition of commercial calcium carbonate (CC) has a high $CaCO_3$ content of 99.35%. The results show that these calcium sources are mainly made of $CaCO_3$. The loss on ignition is 12.36 % by mass in the metakaolin obtained from the kaolin.

It emerges from this table that the chemical composition of commercial calcium carbonate (CC) has a high $CaCO_3$ content of 99.35%. The results show that these calcium sources are mainly made of $CaCO_3$. The loss on ignition is 12.36 % by mass in the metakaolin obtained from the kaolin.

ii. X-ray diffractograms

Figure 6 shows the X-ray diffractogram of eggshell powders (ES). This diffractogram shows the characteristic peaks of calcite ($CaCO_3$).

iii. Thermal analyzes (TGA / DSC) of eggshell powders

Figure 7 shows the DSC and ATG curves of the eggshell powders. We observe on the DSC curve, an endothermic peak around 96 ° C accompanied by a loss of mass on the ATG curve corresponding to the evaporation of adsorbed water [32]. The DSC curve shows an exothermic peak only around 375°C which is accompanied by a low mass loss over that of A TG. This peak is attributable to the decomposition of organic matter [32,33]. The endothermic peak around 622°C on the camber e DSC but not accompanied by any mass loss on the TGA curve suggests that c and accident is not due to a dehydroxylation but the décomposition aragonite in an intermediate amorphous phase [32]. The endothermic peak on the DSC curve at about 906°C is accompanied by a loss of mass on the ATG curve. This phenomenon is attributed to the decomposition of calcium carbonate according to the equation:

$$CaCO_3 \xrightarrow{906°C} CaO + CO_2 \uparrow$$

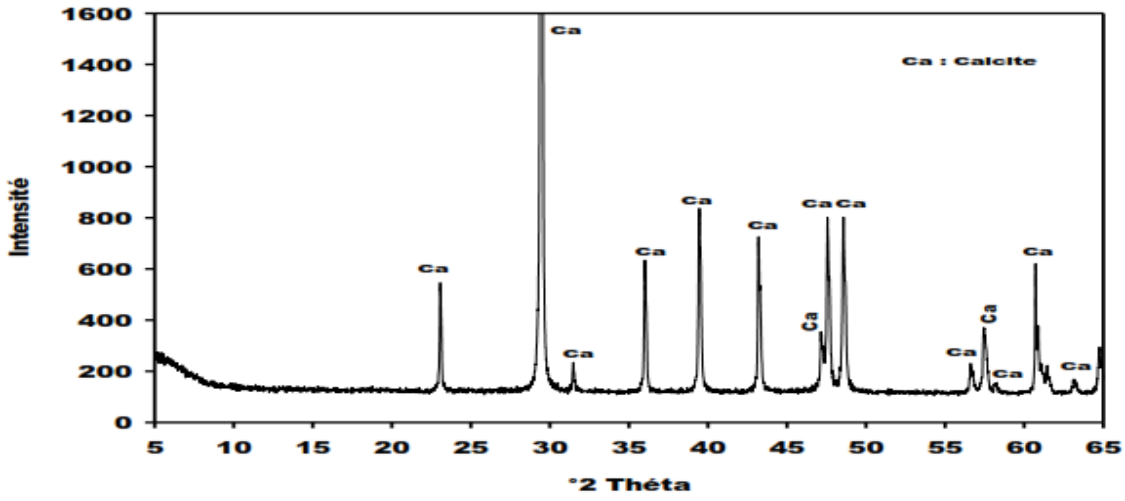

Figure 6. X-ray diffractograms of eggshells (ES)

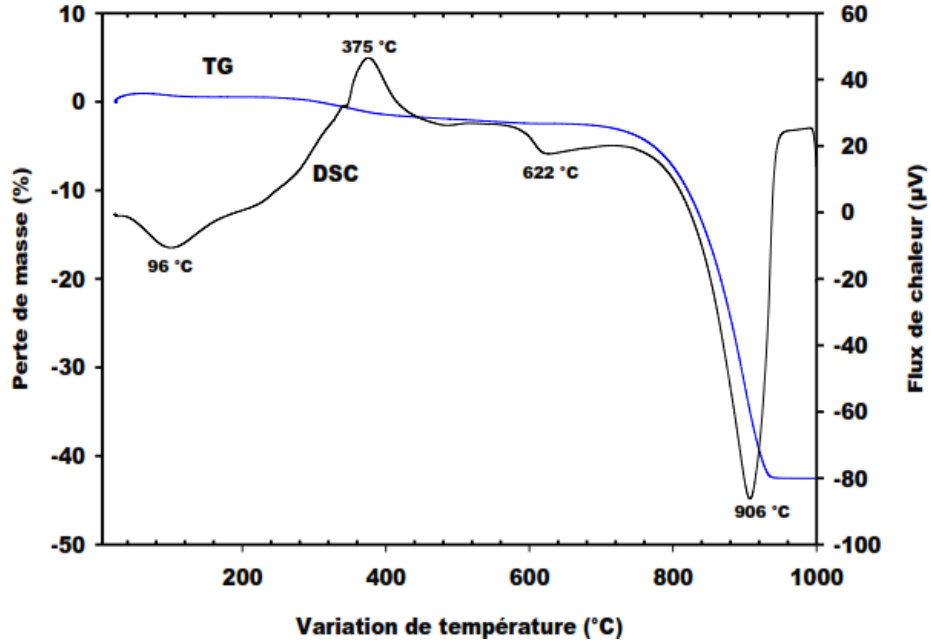

Figure 7. ATG and DSC thermograms of eggshell powders

iv. Infrared spectroscopy

Figure 7 shows the infrared (IR) spectrum of eggshell powders. This spectrum shows the presence of a weak absorption band at 3411 and 1662 cm^{-1}. This is attributable respectively to the OH and H-O-H bonds of the water of hydration molecules. The bands at 780, 2516, 2876, 2983 cm^{-1} are assigned to the modes of vibration of the C = O bonds of carbonate groups [34]. Those at 713, 875 and 1419 cm^{-1} are attributed to the vibrations of elongation of the CO bonds of calcite. The bands at 1156 and 672cm^{-1} are attributable to the CO_3^{2-} ions of aragonite [35]. The band at 594 cm^{-1} is assigned to the O-Ca-O and Ca-O bonds [34,36].

5.3. Characterization of Geopolymer Cements Produced

i. Apparent density

It emerges from these values that the apparent densities of geopolymer cements decrease when the aluminosilicate materials (metakaolin) are replaced by proportions of eggshell powders and commercial calcium carbonate (0, 1, 3, 5, 7 and 10 %). This decrease is due to the ion size of the pores in geopolymeric cement structures and the pore diameters could increase as more eggshell powders are added. Although these values decrease, the values of the bulk densities of the geopolymer cements synthesized are much higher than those obtained by [37,38].

ii. Compressive strengths

It is observed that the compressive strengths of geopolymer cements based on eggshells are greater than those based on commercial calcium carbonate. This would be due to a weak reactivity of calcium carbonate causing rather a precipitation reaction between the dissolved species during the depolymerization of calcium carbonate favoring the formation of the crystalline phases which can consume a large quantity of the PO_4^{3-} ions coming from the 'Phosphoric acid. The increase in compressive strengths when the percentage of eggshell powders increases, would be due to the formation of a large amount

of crystalline phases such as brushite, monetite, newberyte and tricalcium phosphate in the structures of geopolymer cements with 7% incorporation and which could play the role of filler. This result clearly corroborates that of the apparent densities (Table 4) which presents the same phenomenon.

iii. Thermal conductivity

According to the results of the thermal conductivities obtained in Table 6, the thermal conductivity decreases with the increase of the porogen. The decrease in thermal conductivity after bulk addition of the calcium sources is attributed to the formation of pores in these materials due to the emission of CO_2. This result corroborates with that of the apparent density and that of the compressive strength which decreases with the increase of the porogen. We can conclude that the thermal conductivity of porous geopolymer cements obtained from these additives rich in calcium has properties suitable for thermal insulation applications [39] combined fly ash with sodium carbonate and sodium silicate for making of porous geopolymer having a thermal conductivity between 0.29 and 0,34W / mK. While [37] used sawdust to prepare porous geopolymer cements and obtained a thermal conductivity between 0.15 and 0.24W/mK [40] studied the mechanical and thermal properties of a geopolymer mortar lightweight by incorporating granular rubber. They indicated that the thermal conductivities were between 0.237 and 0.298 W/mK. It is important to note that all of these authors used sodium silicate as a hardener. The results obtained in this work are comparable to those obtained by [37].

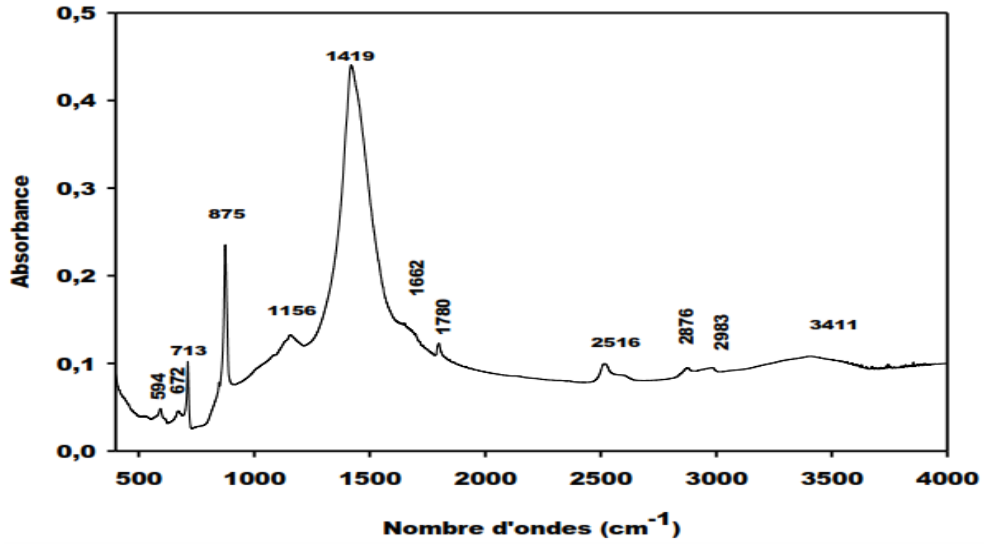

Figure 8. Infrared spectrum of eggshell powders

Table 4. Apparent densities of geopolymer cements based on subtitled metakaolin with eggshells and commercial carbonate

% MKS	0	1	3	5	7	10
Density in g / cm ^{3} with Eggshell	2.37	2.14	1.98	1.84	1.93	1.88
Density in g / cm ^{3} with calcium carbonate	2.18	2.09	1.88	1.89	2.02	1.70

Table 5. Compressive strengths of geopolymer cements based on metakaolin substituted for eggshells (ES) and commercial carbonate (CC)

% MKS	0	1	3	5	7	10
Compressive strengths (MPa) with CC	9.15	11.85	12.07	11.12	34.54	70.17
Compressive strengths (MPa) with ES	9.71	12.18	13.96	12.42	36.22	72.46

Table 6. Thermal conductivity of geopolymer cements based on metakaolin substituted for eggshells and commercial carbonate

% MKS	0	1	3	5	7	10
Thermal conductivity (W / mK) with Eggshell	0.17	0.15	0.12	0.10	0.15	0.15
Thermal conductivity (W / mK) with calcium carbonate	0.26	0.22	0.17	0.14	0.18	0.17

iv. Microstructures

Micro spellings

It can be seen in these Figure 9 and Figure 10 that the MKS0 geopolymer cements based on commercial calcium carbonate are homogeneous, compact and dense, whereas those of MKS0 based on eggshell are heterogeneous and the particles poly (phospho-siloxo) are not well connected to each other. It emerges from these micrographs that the pores are more accentuated on the micrographs of geopolymer cements based on eggshell. It is important to note that during the first stage of geopolymerization in an acidic medium, there is a binding of the proton H from H_3PO_4 to the pair of electrons free of the siloxane or siloxo bond, Si-O-Si [1] according to the following equation:

$$\text{-Si-O-Si -} \xrightarrow[H^+]{H_2PO_4^{2-}} \text{-Si-O-Si-}$$

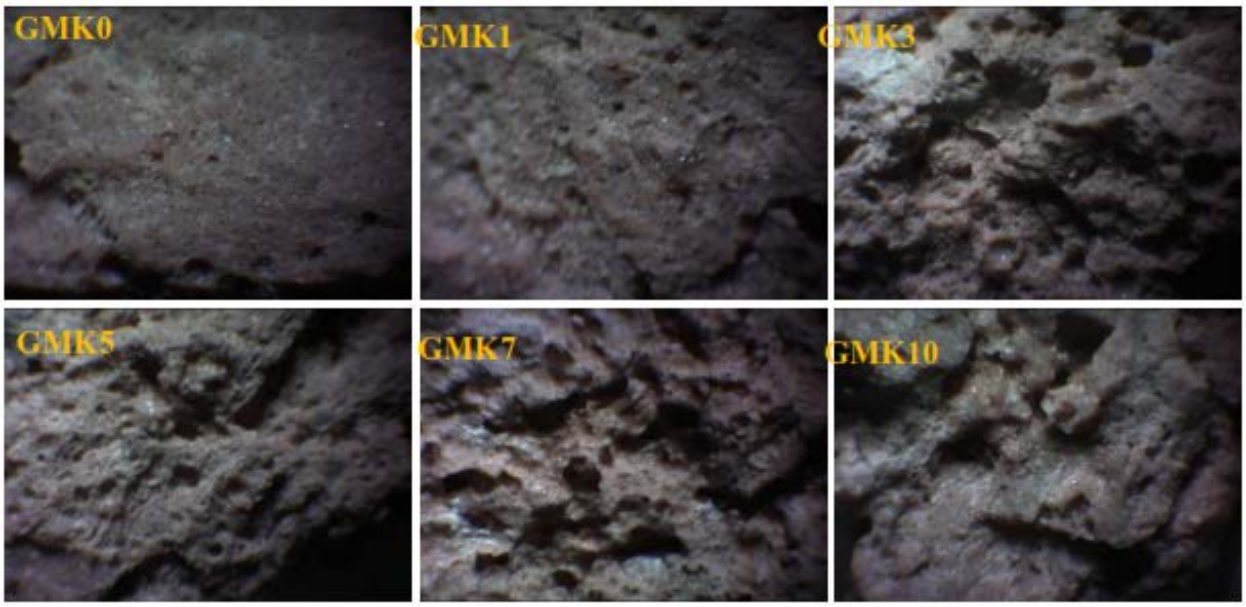

Figure 9. Optical microscopy of geopolymer cements based on metakaolin and eggshells

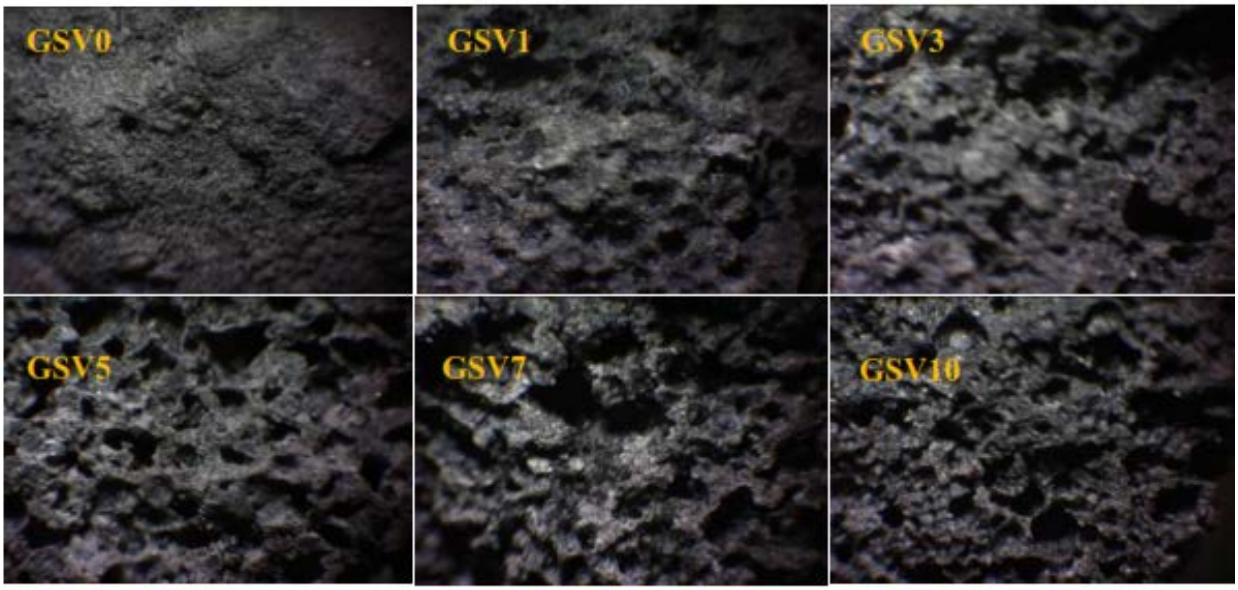

Figure 10. Micrographs of geopolymeric cements based on commercial calcium carbonate

This difference would be due to the fact that the H^+ proton, which fixes the free electron pair of the -Si-O-Si- bond rather reacts with the calcite contained in the eggshell powders. This is causing the formation of pores in the network of geopolymer cements. This was followed by the release of carbon dioxide, oxides such as CaO and MgO contained in commercial calcium carbonate (Table 1) promoting the precipitation of $CaHPO_4$, $Ca_3(PO4)_2$ and $MgHPO_4.3H_2O$. This was contributed to the consumption of phosphate ions thus hampering the depolymerization process on the one hand and polycondensation on the other hand of the Si-OH and Si-OPO $(OH)_2$ species.

v. Mercury intrusion porosimetry (MIP)

According to data reported in Table 7 and Table 8, the volumes of cumulative pore geopolymer cements show that geopolymer cements obtained have accumulated high pores in their structures. These results are in agreement with those of compressive strengths. But, the values of the cumulative pore volumes obtained in this study are higher than those obtained by [41] (between 116 and 179.5 mm^3 /g). It is important to note that these authors replaced up to 40 wt. % of metakaolin with rice husks (pore-forming agent). This difference proves that the nature and quantity of the added pore-forming agent plays a crucial role in the formation of the pores (dimensions, surface area and total volume of the pores) [37]. Replaced metakaolin by volume percentages of sawdust (0, 50, 75, 100, 125, 150, 175 and 200 % by volume) as a pore-forming agent for the synthesis of porous geopolymer cements using a solution of sodium silicate as a hardener. They reported that the cumulative pore volumes were between 180 and 700mm^3/g. This shows that the type of hardener, its concentration and the blowing agent used could significantly influence the pore formation mechanism during the synthesis of porous geopolymer cements.

Table 7. MIP of geopolymeric cements based on eggshell

Samples	Total pore volume (mm^3/g)	Total pore area (m^2/g)	Average pore diameters (nm)	Pore size concentration (nm)
MKS0	213.26	6,243	156.76	290-1440
MKS1	219.67	1,098	192.45	120-4940
MKS3	232.5	7.670	168.78	20,000-39,000
MKS5	279.7	3.981	433.45	10-3950
MKS7	287.41	2.698	532.46	10-6700
MKS10	309.78	2,764	533.78	10-6940

Table 8. MIP of geopolymeric cements based on commercial calcium carbonate

Samples	Total pore volume (mm^3/g)	Total pore area (m^2/g)	Average pore diameters (nm)	Pore size concentration (nm)
MKS0	209,124	6156	167.3	350-1450
MKS1	395.7	2,235	199.8	150-5500
MKS3	355.9	9.147	178.4	25,000-55000
MKS5	399.7	4.327	513.4	10-4500
MKS7	400.1	3.07	643.6	10-8500
MKS10	402.8	3.76	674.9	10 - 9000

Table 9. Total Porosity (MIP), Apparent Densities, Absolute Densities, geopolymer cements based commercial calcium carbonate

Formulations	**MKS 0**	**MKS1**	**MKS3**	**MKS5**	**MKS7**	**MKS10**
Bulk Volumes 1.52 psia (g/mL)	1.46	1.15	1.14	1.24	1.17	1.18
Skeletal Masses (MIP) (g/mL)	2.11	2.11	1.93	2.84	2.17	2.18
Absolute density masses	2.22	2,43	2.42	2.27	2.39	2.37
Open porosity (%)	29.26	39.34	32.55	45.25	41.70	40.56
Closed porosity (%)	5.22	13.26	20.19	0.00	9.14	9.12
Total porosity (%)	34.48	52.60	52.74	45.25	50.84	49.96
Total porosity according to the MIP (%)	30.87	45.35	40.78	45.50	45.89	45.12

Table 10. Total Porosity Values According to MIP, Apparent Densities, Absolute Densities of Eggshell Geopolymer Cements

Formulations	**MKS 0**	**MKS1**	**MKS3**	**MKS5**	**MKS7**	**MKS10**
Bulk Volumes 1.52 psia (g/mL)	1.46	1.15	1.14	1.24	1.17	1.16
Skeletal Masses (MIP) (g / mL)	2.11	2.11	1.93	2.84	2.17	2.12
Absolute density masses	2.22	2,43	2.42	2.27	2.39	2.40
Open porosity (%)	2.926	39.34	32.55	45.25	41.70	40.89
Closed porosity (%)	5.22	13.26	20.19	0.00	9.14	10.32
Total porosity (%)	34.48	52.60	52.74	45.25	50.84	51.25
Total porosity according to MIP (%)	30.87	45.35	40.78	45.50	45.89	45.67

The values of the total porosities calculated with those of the apparent and absolute densities measured using a pycnometer of geopolymer cements are presented in Table 7 and Table 8. Using the bulk density and skeletal density obtained by measuring mercury intrusion porosimetry and absolute density from the helium pycnometer, the open and closed porosities were determined using the formula:

$$\textbf{Total porosity} = \frac{\textbf{Absolute density} - \textbf{Apparent density}}{\textbf{Absolute density}} \textbf{x100}$$

$$\textbf{Closed porosity} = \frac{\textbf{Absolute density} - \textbf{Skeletal density}}{\textbf{Absolute density}} \textbf{x100}$$

From the values recorded in Table 7 and Table 8, it is clear that the total porosity calculated in this case is greater than that obtained by the Porosity intrusion mercury, we can conclude that powders from porous poly(phospho-siloxo) networks could be used for thermal insulation applications.

6. Conclusion

The metakaolin particles in the structure of the final products involve the formation of pores in the network which is confirmed by the high value of the mean pore diameters and the low values of the compressive strengths. The thermal conductivity values obtained suggest that these calcium sources could be used to produce porous geopolymer cements. The values of thermal conductivity, the cumulative volumes of the pores and the total porosities of the porous geopolymer cement obtained by using commercial calcium carbonate as a pore-forming agent are slightly higher than those obtained by using the powders of eggshells. The results show that eggshells can be used as pore-forming agents during the synthesis of porous geopolymer cements that can be used as thermal insulator. The properties of the porous geopolymer cements could be improved for the rest of our work by increasing the concentration of the phosphoric acid solution.

References

[1] Davidovits J. Geopolymer Chemistry and Applications. Third edition, Geopolymer Institute, Saint-Quentin, France (2011) 612.

[2] Wagh AS Chemistry bonded phosphate ceramics-a novel class of geopolymers. Ceramics Transactions 165 (2005) 1007-116.

[3] Cao H., Zhang L., Zheng H., Wang Z. Hydroxyapatite nanocrystals for biomedical applications. The Journal of Physical Chemistry C 114 (2010) 18352-18357.

[4] Tchakouté, KH, Rüscher, CH, Kamseu, E., Djobo, JNY, Leonelli, C. The influence of gibbsite in kaolin and the formation of

berlinite on the properties of métakaolin phosphate-based geopolymer cements. MaterialsChemistry and Physics 199 (2017).
[5] Zhang ZH, Zhu HJ, Zhou CH, Wang H. Geopolymer from kaolin in China: An overview. Applied Clay Science 119 (2015) 31-41.
[6] Ge Y., Yuan Y., Wangliu K. et al. Preparation of geopolymer-based inorganic membrane for removing Ni2 + from wastewater. Journal of HazardousMaterials 299 (2015) 711-718.
[7] Bai C., Franchin G., Elsayed H., Zaggia A., Conte L., Li H., Colombo P. High-porosity geopolymer foams with tailored porosity for thermal insulation and wastewater treatment. Journal of Materials Research 32 (2017) 3251-3259.
[8] Strini A., Roviello G., Ricciotti L., Ferone C., Messina F., Schiavi F., Corsaro D., Cioffi R. TiO $_2$ -based photocatalyticgeopolymers for nitric oxide degradation. Materials 9 (2016) 513p.
[9] Okada K., Imase A., Isobe T., Nakajima A. Capillary rise properties of porous geopolymers prepared by an extrusion method using polylactic acid (PLA) fibers as the pore formers. Journal of the EuropeanCeramic Society 31 (2011) 461-467.
[10] Kumar EM, Ramamurthy K. Influence of production on the strength, density and water absorption of aerated geopolymer paste and mortar using Class F fly-ash. Construction and Buildings Materials 156 (2017) 1137-1149.
[11] Kamseu E., Nait-Ali B., Bignozzi MC, Leonelli C., Rossignol S., DS Smith. Bulk composition and microstructure dependence of effective thermal conductivity of porous inorganic polymer cements. Journal of the EuropeanCeramic Society 32 (2012) 1593-1603.
[12] Font A., Borrachero MV, Soriano L., Monzó José., Payá J. Geopolymer eco-cellular (GECC) based on fluid catalytic cracking catalyst residue (FCC) with addition of recycled aluminum foil powder. Journal of Cleaner Production 168 (2017) 1120-1131.
[13] Luna-Galiano Y., Leiva C., Arenas C., Fernandez-Pereira C. Fly ash-based geopolymeric foams using silica fume as pore generation agent. Physical, mechanical and acoustic properties. Journal of Non-crystalline Solids 500 (2018) 196-204.
[14] Novais RM, Buruberri LH, Ascensao G., Seabra, MP, Labrincha JA Porous biomass fl y ash-based geopolymers with tailored thermal conductivity. Journal of Cleaner Production 119 (2016) 99-107.
[15] Cilla, MS, Morelli, MR, Colombo, P. Open cell geopolymer foams by a novel saponification / peroxide / gel casting combined route. Journal of the EuropeanCeramic Society 34 (2014) 3133-3137.
[16] Vaou V., Panias D. Thermal insulating foamy geopolymers from perlite. Minerals Engineering 23 (2010) 1146-1151.
[17] Abdollahnejad Z., Pacheco-Torgal F., Félix T., Tahri W., Aguiar JB Mix design, properties and cost analysis of fly ash-based geopolymer foam. Construction and Building Materials 80 (2015) 18-30.
[18] Tchakouté KH, Elimbi A., Yanne E., Djangang CN Utilization of volcanic ash for the production of geopolymers cured at ambient temperature. Cement and Concrete Composites 38 (2013) 78-81.
[19] Zhang, Z., Provis, JL, Reid, A., Wang, H. Mechanical, thermal insulation, thermal resistance and acoustic absorption properties of geopolymer foam concrete. Cement and Concrete Composites 62 (2015) 97-105.
[20] Ngouloure ZNM, Nait-Ali B., Zekeng S., Kamseu E., Melo UC, Smith D., Leonelli C. Recycled natural wastes in metakaolin-based porous geopolymers for insulating applications. Journal of Building Engineering 3 (2015) 58-69.
[21] Bell JL, Kriven WM Preparation of ceramic foams from metakaolin-based geopolymer gels. Ceramics Engineering Science Procedure 29 (2009) 97-111.
[22] Shiu, H.-S., Lin, K.-L., Chao, S.-J., Hwang, C.-L., Cheng, T.-W. Effects of foam agent on characteristics of thin-film transistor liquid crystal display waste glass-metakaolin-based cellular geopolymer. Environmental Progress SustainableEnergy 33 (2014) 538-550.
[23] Landi E., Medric V., Papa E., Dedecek J., Klein P., Benito P., Vaccari A. Alkali-banded ceramics tailored porosity. Applied Clay Science 73 (2013) 56-64
[24] Sasmal N., Garai M., Karmakar B. Preparation and characterization of novel foamed porous glass ceramics. Materials Characterization 103 (2015) 90-100.
[25] Fernandes, HR, Ferreira, DD, Andreola, F., Lancellotti, I., Barbieri, L., Ferreira, JMF: Environmental friendly management of CRT glass by foaming with waste egg shells, calcite or dolomite. Ceramics International 40 (2014) 13371-13379.
[26] Gualtieri LM, Romagnoli M., Gualtieri FA Preparation of phosphoric acid-based geopolymer foams using limestone as pore forming agent. Thermal properties by in situ XRPD and Rietveld refinements. Journal of the European Ceramic Society 35 (2015) 3167-3178.
[27] *Department of Geology and Mines 1979*. http://www.worldcat.org/title/carte-geologique-de-reconnaissance-du-cameroun-garoua-ouest/oclc/81788746&referer=brief_results. 15-09-2017.
[28] Laurie Bourgeois. Clay minerals. Polytech, Paris UPMC. P15, 2015.
[29] Sobgwi TE Contribution to the physico-chemical and mineralogical study of materials from the Mayouom clay deposit (West Cameroon): Case of materials from well number 1. Magister'sthesis, University of Yaoundé I, P64, 2005.
[30] Maglione G., Carn M. Infrared spectra of saline minerals and neoformed silicates in the Chad basin. Cah. ORSTOM, Geol., Vol.VII, P3-9, 1975.
[31] Wetshondo Osomba. Characterization and valuation of clay materials from the Province of Kinshasa (DR Congo). Doctoral thesis, University of Liège, Architecture, Geology, 2012.
[32] Bashir ASM, Manusamy Y. Characterization of Raw Egg Shell Powder (ESP) as A Good Bio-filler. Journal of Engineering Research and Technology 2 (2016).
[33] Freire MN, Holanda JNF Characterization of avian eggshell waste aiming its use in ceramic wall tile paste. Ceramica 52 (2006) 240-244.
[34] Anjaneyulu U., Sasikumar S. Bioactive nanocrystallinewollastonite synthesized by sol-gel combustion using eggshell waste as calcium source. Bulletin of Materials Science 37 (2014) 207-212.
[35] Hongxia G., Zhenping, Q., Peng, Q., Peng, Y., Suping C., Wei W. Crystallization of aragonite $CaCO_3$ with complex structures. Advances Powder Technology 22 (2011) 777-783.
[36] Choudhary R., Koppala S., Swamiappan S. Bioactivity studies of calcium magnesium silicate prepared from eggshell waste by sol-gel combustion synthesis. Journal of AsianCeramic Society 3 (2015) 173-177.
[37] Fongang RTT, Pemndje J., Lemougna PN, Melo UC, Nanseu CP, Nait-Ali B., Kamseu E., Leonelli C. Cleaner production of the lightweight insulating composites Microstructure, pore network and thermal conductivity. Energy and Building 107 (2015) 113-122.
[38] Hassan HS, Abdel-Gawwad HA, Vásquez García SR, Israde-Alcántara I. Fabrication and characterization of thermally-insulating coconut ash-based geopolymer foam. Waste Management 80 (2018) 235-240.
[39] Alghamdi H., Neithalath N. Novel synthesis of lightweight geopolymer matrices from fly ash through carbonate-based activation. Materials Today Communications 17 (2018) 266-267.
[40] Wongsa A., Sata, V., Nematollahi B., Sanjayan J., Chindaprasirt. P. Mechanical and thermal properties of lightweight geopolymer mortar incorporating crumb rubber. Journal of Cleaner Production 195 (2018) 1069-1080.
[41] Riyap HI, Bewa CN, Banenzoué C., Tchakouté HK, Rüscher CH, Kamseu E., Bignozzi MC, Cristina Leonelli. Microstucture and mechanical, physical and structural properties of sustainable lightweight metakaolin-based geopolymer cements and mortars employing rice husk. Journal of AsianCeramicSocieties 7 (2019) 199-212.